

## in the Adriatic Sea

I. Martić, N. Degiuli & I. Čatipović

*Faculty of Mechanical Engineering and Naval Architecture, University of Zagreb, Zagreb, Croatia*

**ABSTRACT:** In this paper the ship seakeeping characteristics in regular head waves are calculated. The ship response is calculated at defined sea states for the Adriatic Sea in certain frequency range and at different forward speeds. Since after a maritime accident a damaged ship should be often removed from the place where accident occurred seakeeping characteristics of damaged ship are also calculated. The damage is simulated as the flooded tank within midship area. Determination of ship seakeeping characteristics is then based on coupled motions of ship and fluid inside the tank. Calculations are based on the linear potential flow theory and performed using hydrodynamic software (HydroSTAR 2010). Response amplitudes of the ship are presented using transfer functions. Seakeeping characteristics of the intact and damaged ship are compared. In order to compare the calculated results with experimental data from the literature, motion amplitudes of the ship model are also calculated. The obtained results show that response amplitudes of coupled seakeeping and sloshing motions differ slightly from the amplitudes of intact ship, except in case of surge at low incoming wave frequencies.

### 1 INTRODUCTION

Ship seakeeping characteristics include motion, velocity and acceleration of the ship as result of the navigation in waves. Seakeeping characteristics are affected by environmental conditions, condition of the ship itself and the way of handling and steering the vessel. The ship has good seakeeping characteristics if motion amplitudes are moderate and acceleration is within acceptable limits for the crew, passengers and equipment (Prpić-Oršić & Čorić 2006). Motions and loads are calculated for different sailing routes and sea states that ship will encounter while sailing. It is of great importance to evaluate ship performance particularly at higher sea states. Ship response to actual sea state and possible speed loss is important not only from economic but also an environmental aspect (Prpić-Oršić & Faltinsen 2012). Ship response to waves is usually presented using transfer functions, which describe the amplitudes of ship motions as a function of incoming wave frequency and allow further evaluation of the ship response at certain sea states.

This paper deals with ship response to regular waves in a certain frequency range and by using the resulting transfer functions, the response at the defined sea states is determined. In order to evaluate the influence of fluid motions inside the hull (when damage due to collision or grounding occurs) on global ship motions, flooded internal

tank is generated and the resulting response of the damaged ship is compared with the response to waves of the intact ship.

Sloshing inside the tank can be initiated by incoming waves i.e. the ship motions in waves and it may cause significant load on tank walls. It also affects the global ship motions.

Effect of sloshing inside the tanks is often linearized in ship motion analysis. It is necessary to satisfy the Laplace equation and boundary condition on tank walls in order to approximate sloshing by using the linear potential theory. If the tank is equipped with slosh-suppressing devices, the fluid motions can be quite accurately modelled by using linear theories (Gavrilyuk et al. 2005). In certain frequency range, significant nonlinearity can occur caused by coupling of tank liquid and ship motions (Li et al. 2014). There are two approaches to solve sloshing hydrodynamic problem: in frequency domain based on the linear potential flow theory and in time domain based on the non-linear viscous flow theory (Li et al. 2014). Fluid motions inside the tank generate severe hydrodynamic loads that can violate structural integrity and stability and put in danger the whole ship. The ship motions affected by the coupling are the surge, sway, roll and yaw motions (Diebold et al. 2008).

Since in this paper only head waves were imposed on the ship the effect of coupling is investigated only for surge, heave and pitch motions in frequency domain.

## 2 MOTION CALCULATIONS USING LINEAR THEORY

In order to simulate the fluid flow around the ship when sailing as simply as possible with satisfactory suitability, the linear potential flow theory based on Laplace equation is used:

$$\Delta\varphi = 0 \quad (1)$$

where velocity potential  $\varphi$  is defined in fluid domain. The potential  $\varphi$  should also fulfil following boundary conditions:

$$-k\varphi + \frac{\partial\varphi}{\partial z} = 0 \quad \text{on } z = 0 \quad (2)$$

and on the wetted surface:

$$\frac{\partial\varphi}{\partial n} = v_n \quad (3)$$

where  $k$  = wave number,  $n$  = unit surface normal of boundary element and  $v_n$  = collocation point velocity.

Within this approach the condition on the outgoing waves is formulated according to Sommerfeld condition:

$$\lim_{R \rightarrow \infty} \left[ \sqrt{kR} \left( \frac{\partial\varphi}{\partial R} - ik\varphi \right) \right] = 0 \quad (4)$$

The flow around the hull is analyzed using two models: the incoming waves acting on a stationary body and body that oscillates in a calm fluid (Prpić-Oršić & Čorić 2006). Knowing the flow velocity potential it is possible to determine the velocity and acceleration of fluid particles, hydrostatic and hydrodynamic pressure acting on a given depth and wave energy. Coupled motions are of great importance in determining the ship global motions and loads. Motion amplitudes (and velocity and acceleration amplitudes as partial derivatives of motion functions) are determined by linear superposition of ship harmonic motions. Vertical motions have only slight effect on transverse ones due to the symmetry of the ship about the longitudinal axis. But on the other hand the transverse ship motions have significant influence on the motions, forces and moments in the vertical plane (Prpić-Oršić & Čorić 2006).

In linear theory it is assumed that the relation between the hydrostatic force and ship motion is linear, and hydrostatic force is caused only due to buoyancy changes. In nature, nonlinearity of ship motions due to hydrostatic forces is most conspicuous in case of roll. In potential flow theory,

damping refers to the dissipation of energy of the ship radiation waves and it is called potential damping. Viscous damping due to friction between layers of fluid is negligible in the case of all ship motions except for roll (Prpić-Oršić & Čorić 2006).

## 3 S-175 CONTAINER SHIP RESPONSE TO WAVES

### 3.1 S-175 container ship

To compare the experimentally obtained results of the ship response to waves with those calculated numerically, the S-175 container ship model test data were used (Nakayama 2012). Tests were conducted on a stationary model and at three different speeds. Regular head waves ( $180^\circ$ ) of 30 mm wave height and different ratios of wavelengths and the length of the model  $\lambda/L$  were generated. The principal dimensions of the full scale S-175 container ship and its model are given in Table 1 and the body plan is shown in Figure 1. The hull mesh created using hydrodynamic software (HydroSTAR

Table 1. Principal dimensions of the S-175 container ship.

	Full scale	Model
Length, $L$ (m)	175.0	3.0
Breadth, $B$ (m)	25.4	0.435
Draft of fore peak $T_F$ (m)	7.0	0.120
Draft of midship $T$ (m)	9.50	0.163
Draft of aft peak $T_A$ (m)	12.02	0.206
Displacement volume, $\nabla$ (m <sup>3</sup> )	24154.13	0.122
Block coefficient, $C_B$	0.572	0.572
Position of LCG, $x_G$ (m)		-0.141
Radius of gyration, $k_{yy}/L$		0.239

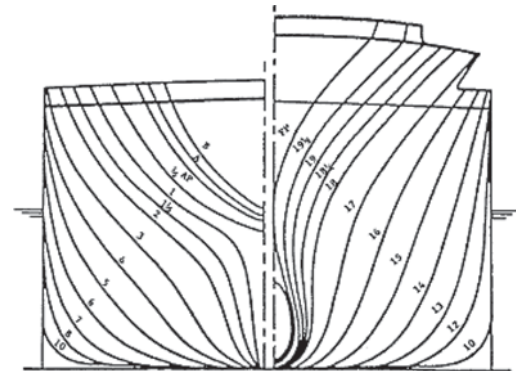


Figure 1. Body plan of the S-175 container ship (Nakayama 2012).

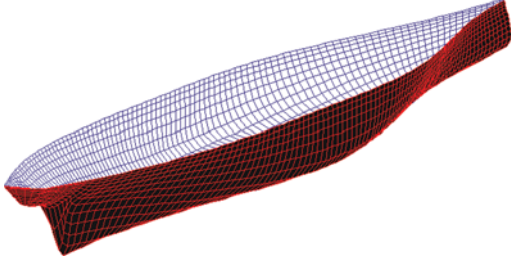


Figure 2. Panel model of the S-175 container ship, (HydroSTAR 2010).

2010) is shown in Figure 2. The software is based on the linear potential flow theory and it provides calculations of motions and loads of first and second order. It requires the input parameters of ship model and waves characteristics. It uses boundary integral equations in solving the seakeeping and sloshing hydrodynamic problems and provide determination of diffraction and radiation potentials (HydroSTAR 2010). Since it is based on potential flow, a fictitious force is added in momentum equations in order to take into account the energy dissipation and damping to avoid unlimited responses at resonant frequencies.

#### 4 INFLUENCE OF FLOODED INTERNAL TANK ON GLOBAL SHIP MOTIONS

The fluid inside the hull has influence on ship global loads and motions during navigation. It is therefore necessary to estimate the effect of motions and loads of liquid inside the tanks. It is also necessary to know the ship response to waves in damaged condition for a particular sea state. Determination of seakeeping characteristics in that case is based on coupled motions of a ship as a rigid body and fluid inside the tank. Mentioned hydrodynamic problem can also be solved under the assumptions of the linear potential flow theory. Sloshing and seakeeping parts are considered separately.

The movement of liquid inside the tank has six degrees of freedom like the ship and as well as in the ship seakeeping part, the boundary integral equation based on the so called source formulation is used to solve the hydrodynamic problem (Malenica et al. 2003). Since the linear potential theory is considered, there is no damping generated by the liquid motions within the tanks. Solving the hydrodynamic motion and load within the flooded tanks provides additional members in added mass matrix associated with each tank motion and matrix of hydrostatic restoring forces (Malenica et al. 2003). Motions, forces and moments of liquid inside the

tanks are described and solved in the local coordinate system. Therefore they need to be transformed to the ship global coordinate system. The dynamic equilibrium equation valid for the global coordinate system of the coupled ship and tank matrices can be written as follows (Malenica et al. 2003):

$$\begin{aligned} & \left( -\omega^2 \left( [M_Q] + [A_Q] + [A_T] + [A_{TQ}] \right) - i\omega [B_Q] \right) \\ & + \left( [C_Q] + [C_T] + [C_{TQ}] \right) \{ \eta_j \} = \{ F_Q \} \end{aligned} \quad (5)$$

where  $[M_Q]$  = mass matrix;  $[A_Q]$ ,  $[A_T]$  = hydrodynamic added mass matrix;  $[B_Q]$  = hydrodynamic damping matrix;  $[C_Q]$ ,  $[C_T]$  = hydrostatic restoring matrix;  $[A_{TQ}]$ ,  $[C_{TQ}]$  = transfer matrices from the point  $T$  to the point  $Q$ ;  $\eta_j$  = ship motions;  $F_Q$  = hydrodynamic excitation force; subscript “ $Q$ ” indicates that matrix is written with respect to global reference point  $Q$  and subscript “ $T$ ” to tank reference point  $T$ .

Hydrostatic forces and moments acting on the ship should be determined by integrating the pressure along the wetted surface area. For seakeeping part liquid inside the tank is considered to be a rigid part of the ship. Hydrodynamic loads can be determined based on the potential flow velocity of incoming wave and its diffraction component, as well as radiation potentials of ship motion. In the case of the fluid motions inside a tank similar procedure is used to determine the hydrodynamic and hydrostatic loads as previously mentioned. Since the free surface of a fluid inside the tank is always horizontal according to linear theory, a correction of vertical coordinates is used in the integration of pressure along the wetted surface area of tank walls in order to determine hydrostatic pressure. The calculations are carried out considering the centre of the free surface of liquid in the tank. Since liquid inside the tank is considered a rigid mass when solving seakeeping part, that contribution needs to be subtracted by fictive mass restoring matrix. Global restoring of coupled system is then reduced (Malenica et al. 2003).

The difference between solving hydrodynamic problems of the ship and the liquid inside the tank is the absence of diffraction potential in the tank and different boundary conditions at the free surface since the free surface of the fluid inside the tank moves along with the ship, Figure 3.

Dynamic and kinematic boundary conditions are defined as follows:

$$\frac{\partial \xi}{\partial t} = \frac{\partial \Phi}{\partial z} \quad (6)$$

$$-\rho g (\xi - Z_v^A) - \rho \frac{\partial \Phi}{\partial t} = 0 \quad (7)$$

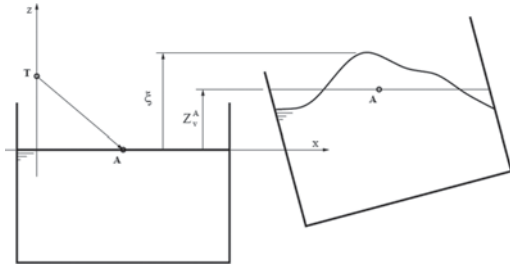


Figure 3. Motion of the free surface inside the tank (Malenica et al. 2003).

where  $\xi$  = free surface elevation defined according to initial calm condition;  $\Phi$  = flow velocity potential;  $\rho$  = fluid density;  $g$  = gravity acceleration;  $Z_v^A$  = vertical displacement of the centre of waterplane area.

Combining the mentioned boundary conditions it can be written:

$$\frac{\partial^2 \Phi}{\partial t^2} + g \frac{\partial \Phi}{\partial z} = g \frac{\partial Z_v^A}{\partial t} \quad (8)$$

After substitutions  $\Phi = \text{Re}\{\varphi e^{-i\omega t}\}$  and  $Z_v^A = \text{Re}\{\xi_v^A e^{-i\omega t}\}$  in frequency domain, the boundary condition becomes:

$$-\nu \varphi + \frac{\partial \varphi}{\partial z} = -i\omega \xi_v^A \quad (9)$$

With respect to the potential theory there is no damping present, so the problem of resonant frequencies of fluid motion inside the tank may occur and unrealistic responses to these frequencies are possible (Malenica et al. 2003). It is therefore necessary to correct this model of determination of coupled motions/responses of the ship and the liquid inside the tank by at least approximate damping factors which may be based on empirical data or experimental tests. The parameter for the correction of damping inside the tanks is determined through comparison with experimental data (Diebold et al. 2008). The basic idea is the correction of boundary conditions on the tank walls by some factors in order to create the main energy dissipation in the tank boundaries. To describe the fluid motions of internal tanks due to ship motions in waves is a very complex process and it cannot be described using linear theory. According to (Malenica et al. 2003) the motion of the liquid inside the tank cannot be simulated even by nonlinear potential theories with sufficiently accuracy, but more complex models must be used (e.g. a model based on the Navier-Stokes equations). However, for the estimation purpose of the influence that liquid inside the

tank has on global ship motions, potential theory gives satisfactory results.

In order to simulate the mentioned hydrodynamic problem, a flooded tank due to damage of the S-175 container ship was generated, Figure 4. The volume of fluid in the tank is 48.49% of the displacement volume of intact ship ( $T = 12.01667$  m), or 32.74% of the displacement volume of the ship immersed for  $\Delta T = 3.483$  m after the flooding. The first attempt of simulating the damaged ship was to create a flooded internal tank of the volume displacement equal to about 10% of the ship volume displacement. Since that model did not give almost any difference in transfer function comparison, a much larger tank was generated in order to create distinctive responses. Characteristics of generated midship tank are shown in Table 2 and damaged ship hydrostatic characteristics in Table 3.

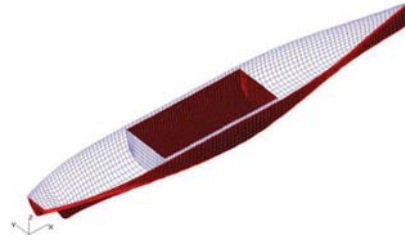


Figure 4. Mesh of the S-175 container ship with internal tank, (HydroSTAR 2010).

Table 2. Tank characteristics.

Length, $L_T$ (m)	54.75
Maximum width, $B_T$ (m)	22.0
Longitudinal position (m)	$x_1 = 48.405, x_2 = 103.155$
Displacement volume, $V_T$ (m <sup>3</sup> )	12018
Displacement mass, $\Delta_T$ (m)	12318.45
Waterline area, $A_{WL,T}$ (m <sup>2</sup> )	1204.5
Centre of gravity, $CG_T$ (m)	$x_G = 75.78, y_G = 0,$ $z_G = 10.18$

Table 3. Hydrostatic characteristics of damaged ship.

Draught, $T$ (m)	15.5
Displacement volume, $\nabla$ (m <sup>3</sup> )	36705
Wetted surface area, $S$ (m <sup>2</sup> )	6790.1
Waterline area, $A_{WL}$ (m <sup>2</sup> )	3603.6
Centre of gravity, $CG$ (m)	$x_G = 77.745, y_G = 0,$ $z_G = 15.439$
Centre of buoyancy, $CB$ (m)	$x_B = 77.745, y_B = 0,$ $z_B = 9.711$
Gyration radii (m)	$r_{xx} = 48.405, r_{yy} = 103.155,$ $r_{zz} = 103.155$

## 5 RESULTS

### 5.1 Comparison of the S-175 container ship model transfer functions with experimental data

To compare the calculated ship response to regular waves with experimental data from the literature (Nakayama 2012), motion amplitudes of the S-175 container ship model were determined using hydrodynamic software (HydroSTAR 2010) for the Froude number  $F_r = 0.087$  corresponding to model velocity  $v_M = 0.472$  m/s. All motion calculations have been conducted with respect to the ship centre of gravity. Since only the head waves were generated, significant amplitudes occur only for surge  $\eta_1$ , heave  $\eta_3$ , and pitch  $\eta_5$  motions.

A comparison between experimental data and numerically obtained dimensionless motion amplitudes for a range of wavelength and length of model ratio equal to  $\lambda/L = 0.3$ – $2.0$  is shown in Figures 5–7.

Surge amplitudes of the container ship model increase with the increase of the ratio  $\lambda/L$  i.e. with the decrease of wave frequency. Along with the increase of response amplitudes, deviations between experimental and calculated data are becoming larger. However, motion amplitudes obtained experimentally are only slightly higher than those obtained by using hydrodynamic software (HydroSTAR 2010).

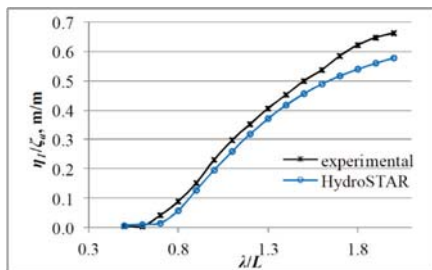


Figure 5. Comparison of surge transfer functions.

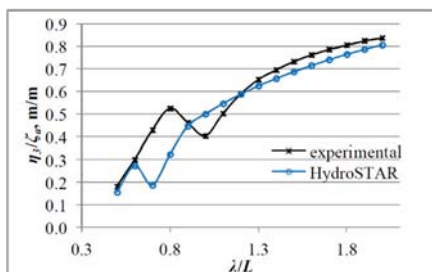


Figure 6. Comparison of heave transfer functions.

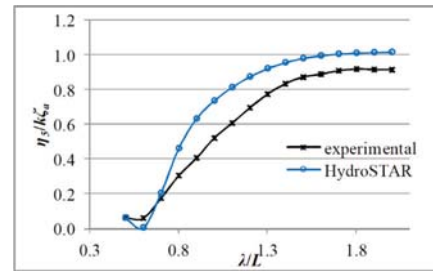


Figure 7. Comparison of pitch transfer functions.

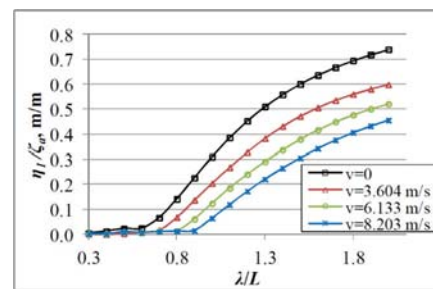


Figure 8. Intact ship transfer functions for surge.

In the case of heave, it is evident that for certain frequencies or ratios  $\lambda/L$ , there are significant deviations between the calculated response amplitudes and experimental data ( $\lambda/L = 0.7; 0.8; 1.0$ ). Local extremes of these two transfer functions occur at different ratio  $\lambda/L$  and there is a significant difference between response amplitudes in certain ratio  $\lambda/L$  range. The numerical method of calculation of radiation and incoming wave loads obviously does not provide enough accurate results for certain i.e. short wavelengths.

In the case of pitch, the calculated amplitudes are higher than experimental data for almost all wavelengths of specified  $\lambda/L$  range.

The maximum deviations between two transfer functions are around 30–35% for the ratios in the range  $\lambda/L = 0.8$ – $1.0$ .

### 5.2 Response to waves of the intact S-175 container ship

In order to calculate the ship response to waves, the head waves were imposed on the S-175 container ship. The analysis was conducted for four Froude numbers ( $F_r = 0; 0.087; 0.148; 0.198$ ) i.e. for stationary ship as well as for three different speeds using hydrodynamic software (HydroSTAR 2010). Obtained transfer functions for different wavelengths are shown in Figures 8–10.



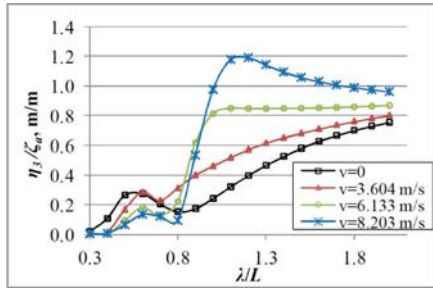


Figure 9. Intact ship transfer functions for heave.

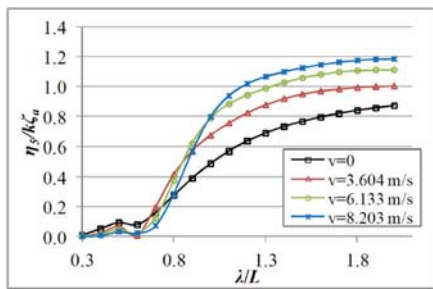


Figure 10. Intact ship transfer functions for pitch.

Transfer functions for surge show a decrease of response amplitudes as the speed increases. Also by increase of speed, frequencies of incoming waves at which the response amplitudes become almost negligible are getting lower. At low frequencies transfer functions converge to one. As speed increases, response amplitudes for heave are also increasing at lower incoming wave frequencies. Resonant frequencies occur at lower incoming wave frequencies which is most evident at highest considered ship speed. Local maximums of transfer heave functions correspond to coupled heave and pitch motions.

The largest pitch motions occur at zeroes of profile function of long incoming waves. According to transfer functions for pitch, response amplitudes decrease as incoming wave frequencies increase. At lower frequencies, response amplitudes are higher if ship speed increases.

### 5.3 Comparison of transfer functions of intact and damaged ship

In order to show the difference between the seakeeping characteristics of the damaged ship condition and the initial intact condition for all speeds, the comparison of obtained transfer functions is made. Fluid inside the tank was first treated as the ship added displacement mass but without affecting the global motions and loads. After that, the

ship seakeeping characteristics were calculated considering also the sea water inside the tank in order to determine the impact of motions and loads of liquid in the tank on global ship motions. Surge, heave and pitch motions are considered and it is obvious that there are no significant differences between these transfer functions. In the case of heave motion of damaged ship at  $v = 0$  there is a higher peak at low ratio  $\lambda/L$ . The same thing can be observed in the case of surge motions at higher ratio  $\lambda/L$ , i.e. at low frequencies for all considered Froude numbers. For the practical reasons, only comparison of transfer functions for stationary ship and for highest speed is shown in Figures 11–16.

### 5.4 Response of the S-175 container ship at defined sea states

In order to estimate the ship response to sea conditions characteristic for the Adriatic Sea, Tabain wave spectrum was used. Tabain wave spectrum is defined as:

$$S_{\zeta}(\omega) = 0.862 \frac{0.0135g^2}{\omega^5} e^{\left[ -\frac{5.186}{\omega^4 H_{1/3}^2} \right]} 1.63^p \quad (10)$$

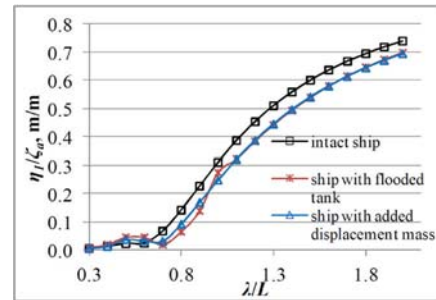


Figure 11. Comparison of transfer functions for surge at  $v = 0$ .

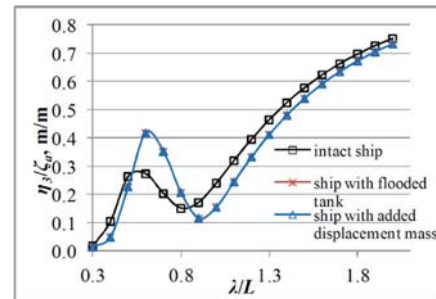


Figure 12. Comparison of transfer functions for heave at  $v = 0$ .

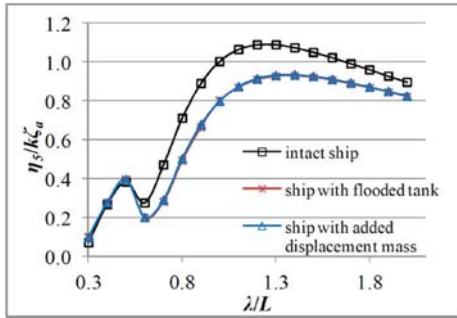


Figure 13. Comparison of transfer functions for pitch at  $v = 0$ .

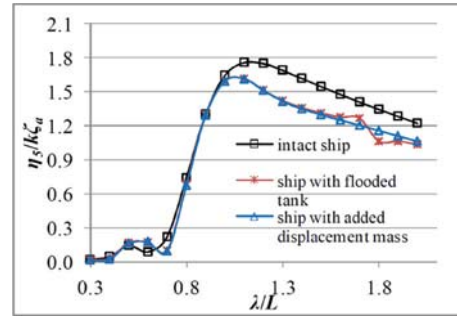


Figure 16. Comparison of transfer functions for pitch at  $v = 8.203$  m/s.

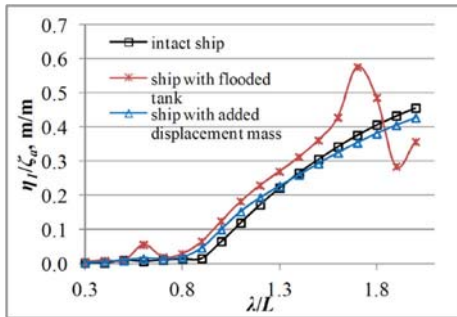


Figure 14. Comparison of transfer functions for surge at  $v = 8.203$  m/s.

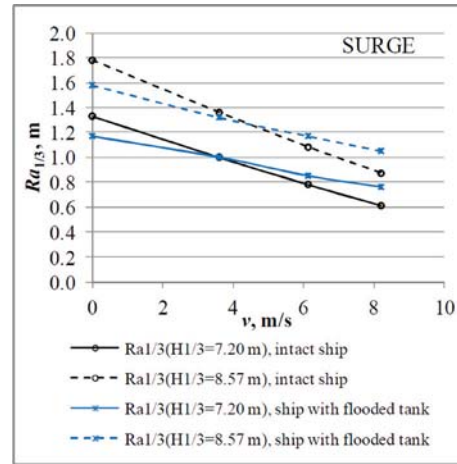


Figure 17. Significant response amplitudes for surge.

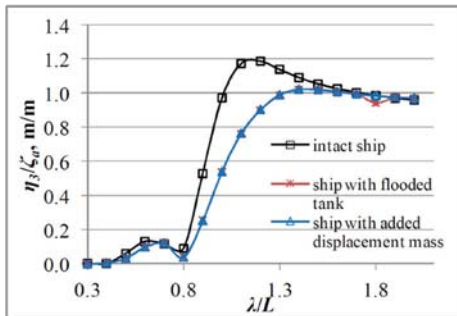


Figure 15. Comparison of transfer functions for heave at  $v = 8.203$  m/s.

where:

$$p = e^{-\left[ \frac{(\omega - \omega_m)^2}{2\sigma^2 \omega_m^2} \right]} \quad (11)$$

$$\omega_m = 0.32 + \frac{1.8}{H_{1/3} + 0.60} \quad (12)$$

$$\sigma = \begin{cases} 0.08 & \text{for } \omega \leq \omega_m \\ 0.1 & \text{for } \omega > \omega_m \end{cases} \quad (13)$$

According to theoretical predictions for the Adriatic Sea the most likely maximum significant wave height for the return period of 20 years is 7.20 m and 8.57 m for the return period of 100 years (Parunov & Senjanović 2005). The analysis was conducted for the mentioned significant wave heights.

Using the ship response energy spectrum it is possible to determine significant response amplitudes for certain sea state. These amplitudes should be determined on the basis of the zeroth spectral moment  $m_{0R}$  i.e. the area under the response spectrum function (Journée & Massie 2001) as follows:

$$R_{a1/3} = 2\sqrt{m_{0R}} \quad (14)$$

The obtained results are shown in Figures 17–19 for surge, heave and pitch.

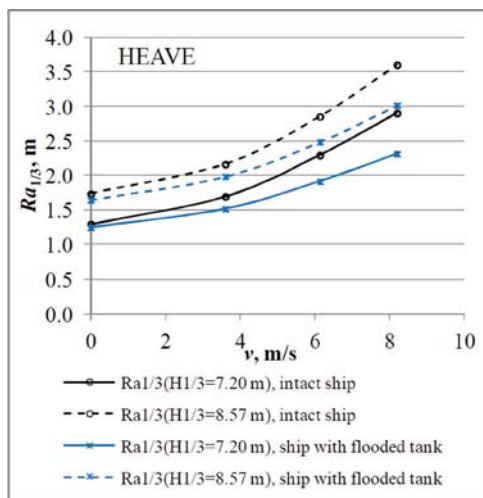


Figure 18. Significant response amplitudes for heave.

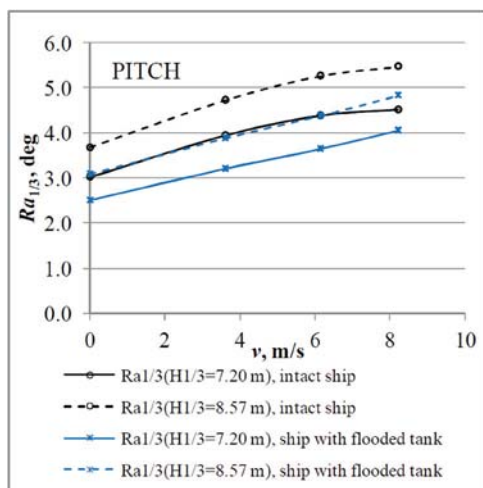


Figure 19. Significant response amplitudes for pitch.

## 6 CONCLUSION

Ship response to waves is determined in the frequency domain assuming potential flow and using linear theory. Due to the reduced natural frequency and increased displacement mass of the damaged ship, response amplitudes decrease compared to the ones of the intact ship. Differences in the response of the damaged and the intact ship are becoming somewhat larger for higher Froude numbers. Coupled motions of the ship as rigid body and the liquid inside the tank, do not show a significant difference compared to intact ship motions except in

the case of surge at low frequencies and long waves. Motions of the liquid inside the tank have almost no influence on the ship heave and pitch motions. In case of heave there is no deformation of the free surface in the tank, so such results were expected. Since the modelling of liquid motions inside the tank is extremely complex, it is difficult to describe this hydrodynamic problem by using the linear potential theory. It is considered that the linear theory takes into account well enough the influence of motions of the fluid inside the tanks on global motions and loads. However, simplifications that the linear potential flow theory assumes and basic damping parameters may underestimate that influence.

## ACKNOWLEDGMENTS

This work has been supported in part by Croatian Science Foundation under the project 8658.

## REFERENCES

- Diebold, L., Baudin, E., Henry, J., Zalar, M. 2008. Effects on sloshing pressure due to the coupling between seakeeping and tank liquid motion. *Proceedings of the 23rd International Workshop on Water Waves and Floating Bodies*, 23rd IWWWFB, Jeju, Korea.
- Gavrilyuk, I.P., Lukovsky, I.A., Timokha, A.N. 2005. Linear and nonlinear sloshing in a circular conical tank. *Fluid Dynamics Research—FLUID DYN RES*, vol. 37, No. 6, pp. 399–429.
- HydroSTAR for Experts. v6.11. 2010. Bureau Veritas, Paris.
- Journée, J.M.J., Massie W.W. 2001. *Offshore Hydro-mechanics*. Delft University of Technology, Delft, Netherlands.
- Li, X., Zhang, T., Zhang, Y., Wang, Y. 2014. Numerical analysis of ship motion coupled with tank sloshing. *Oceans 2014 MTS/IEEE Conference Proceedings*, Taipei, Taiwan, April 7–10.
- Malenica, Š., Zalar, M., Chen, X.B. 2003. Dynamic coupling of seakeeping and sloshing. *Proceedings of The Thirteenth (2003) International Offshore and Polar Engineering Conference*, 13th ISOPE Conference, Honolulu, Hawaii, USA, May 2003, pp. 486–492.
- Nakayama, Y., Yasukawa, H., Hirata, N. and Hata, H. 2012. Time Domain Simulation of Wave-induced Motions of a Towed Ship in Head Seas. *Proceedings of the Twenty-second (2012) International Offshore and Polar Engineering Conference*, Rhodes, Greece, June 2012, pp. 901–907.
- Parunov, J. & Senjanović, I. 2005. Wave loads on oil tankers in the Adriatic sea, *Proceedings of the 1st Conference on Marine Technology in memoriam of the academician Zlatko Winkler*, Rijeka, Croatia, pp. 98–111.
- Prpić-Oršić, J. & Čorić, V. 2006. *Pomorstvenost plovnih objekata*, Zigo, Rijeka, Croatia.
- Prpić-Oršić, J. & Faltinsen, O.M. 2012. Estimation of ship speed loss and associated CO<sub>2</sub> emissions in a seaway, *Ocean Engineering*, Vol. 44, No-1, pp. 1–10.